

Search for emission of unstable ^8Be clusters from hot ^{40}Ca and ^{56}Ni nuclei

M. Rousseau^a, C. Beck^a, C. Bhattacharya^{a,e}, V. Rauch^a, O. Dorvaux^a, K. Eddahbi^a, C. Enaux^a, R.M. Freeman^a, F. Haas^a, A. Hachem^c, D. Mahboub^f, E. Martin^c, P. Papka^a, S.J. Sanders^d, O. Stezowski^g, A. Szanto de Toledo^b, and S. Szilner^a

a) *Institut de Recherches Subatomiques, F-67037 Strasbourg, Cedex 2, France*

b) *Instituto de Física da Universidade de São Paulo, São Paulo, Brazil*

c) *Université de Nice-Sophia-Antipolis, Nice, France*

d) *University of Kansas, Lawrence, KS 66045, USA*

e) *Present address : VECC Calcutta, India*

f) *University of Surrey, Guildford, UK*

g) *Institut de Physique Nucléaire de Lyon, Lyon, France*

ABSTRACT : *The possible occurrence of highly deformed configurations is investigated in the ^{40}Ca and ^{56}Ni di-nuclear systems as formed in the $^{28}\text{Si} + ^{12}\text{C}$ and $^{28}\text{Si} + ^{28}\text{Si}$ reactions, respectively, by using the properties of emitted light charged particles. Inclusive as well as exclusive data of the heavy fragments ($A \geq 6$) and their associated light charged particles (p , d , t , and α -particles) have been collected at the IReS Strasbourg VIVITRON Tandem facility with two bombarding energies $E_{\text{lab}}(^{28}\text{Si}) = 112$ and 180 MeV by using the ICARE charged particle multidetector array, which consists of nearly 40 telescopes. The measured energy spectra, velocity distributions, in-plane and out-of-plane angular correlations are analysed by Monte Carlo CASCADE statistical-model calculations using a consistent set of parameters with spin-dependent level densities. Although significant deformation effects at high spin are needed, the remaining disagreement observed in the $^{28}\text{Si} + ^{12}\text{C}$ reaction for the S evaporation residue suggests an unexpected large unstable ^8Be cluster emission of a binary nature.*

I. INTRODUCTION

The formation and decay processes of **light** di-nuclear systems (in the $A_{CN} \leq 60$ mass region), produced by low-energy ($E_{\text{lab}} \leq 7$ MeV/nucleon) heavy-ion reactions, has been studied for a long time both from the experimental and the theoretical points of view [1]. In most of the reactions studied, whereas the general conclusions about the formation probability for the compound nucleus (CN) and the characteristic features of its decay could clearly be drawn, the properties of the observed fully energy damped yields are still debated in terms of either a fusion-fission (FF) mechanism [1,2,3], which may be considered as the emission of complex (or intermediate mass) fragments, or a deep-inelastic (DI) orbiting [4] mechanism behavior, the latter being found to be particularly competitive in the $^{28}\text{Si}+^{12}\text{C}$ reaction [5]. Since many of the conjectured features for orbiting yields are similar to that expected for the FF mechanism, it is difficult to fully discount FF as a possible explanation for the large energy damped $^{28}\text{Si}+^{12}\text{C}$ yields [4,5] and, thus, FF, DI orbiting, and even

molecular-resonance behavior may coexist in the large-angle yields of the $^{28}\text{Si}+^{12}\text{C}$ reaction [1].

Superdeformed (SD) rotational bands have been found in various mass regions ($A = 60, 80, 130, 150$ and 190) and, very recently, one SD band has also been discovered in the $N = Z$ nucleus ^{36}Ar [6]. This new result makes that the $A \approx 40$ mass region is of special interest for the nuclear γ -ray spectroscopists. With this respect the study of the $N = Z$ nucleus ^{40}Ca is relevant. Since the detection of light charged particles (LCP) is relatively simple, the analysis of their spectral shapes is another good tool in exploring nuclear deformation and other properties of hot rotating nuclei at high angular momenta. Experimental evidence for angular momentum dependent spectral shapes has already been widely discussed in the literature [7-11]. Thus we decided to investigate the ^{40}Ca nucleus produced through the $^{28}\text{Si} + ^{12}\text{C}$ reaction at the following bombarding energies $E_{lab}(^{28}\text{Si}) = 112$ and 180 MeV. Data have also been collected for the $^{28}\text{Si} + ^{28}\text{Si}$ reaction (leading to the $N = Z$ nucleus ^{56}Ni) in the same experimental conditions.

II. EXPERIMENTAL RESULTS

A. Experimental techniques :

The experiments were performed at the IReS Strasbourg VIVITRON Tandem facility using 112 MeV and 180 MeV ^{28}Si beams which were incident on ^{12}C (160 and 180 $\mu\text{g}/\text{cm}^2$ thick) and ^{28}Si (180 and 230 $\mu\text{g}/\text{cm}^2$ thick) targets mounted in the ICARE scattering chamber [12]. Both the heavy ions ($A \geq 6$) and their associated LCP's (p, d, t, and α) were detected using the **ICARE** charged particle multidetector array [12] which consists in nearly 40 telescopes in coincidence. The heavy fragments, i.e. ER, quasi-elastic (QE), DI, and FF fragments, were detected in 10 heavy-ion telescopes, each consisting of an ionisation chamber (IC) followed by a silicon surface-barrier diode of 500 μm effective thickness. Both the in-plane and out-of-plane coincident LCP's were detected using either 3 three-elements light-ion telescopes (Si 40 μm , Si 300 μm , CsI(Tl) 2 cm) or 24 two-elements light-ion telescopes (Si 40 μm , CsI(Tl) 2 cm) and two light-ion telescopes (IC, Si 500 μm) located at the most backward angles. The CsI(Tl) scintillators were coupled to photodiode readouts. The IC's were filled with isobutane and the pressures were kept at 30 torr and at 60 torr for detecting heavy fragments and light fragments, respectively. The acceptance of each telescope was defined by thick aluminium collimators. The distances of these telescopes from the target ranged from 10.0 to 30.0 cm, and the solid angles varied from 1.0 msr at the most forward angles to 5.0 msr at the backward angles.

The different energy calibrations of the ICARE multidetector array have been done using radioactive sources in the range of 5 to 9 MeV, a precision pulser, elastic scattering yields from ^{28}Si on ^{197}SAu , ^{28}Si and ^{12}C targets, and data from the $^{16}\text{O}+^{12}\text{C}$ reaction measured at $E_{lab} = 53$ MeV [12]. In this last case, α -particles emitted in the $^{12}\text{C}(^{16}\text{O},\alpha)^{24}\text{Mg}^*$ reaction provide known energies from ^{24}Mg excited states and allow for the α -particle calibration of the backward angle detectors. The proton calibration was done with scattered protons from Formvar targets in reverse kinematics reactions with both ^{28}Si and ^{16}O beams.

B. Experimental data :

The inclusive cross sections for C, N and O fragments produced in the $^{28}\text{Si}+^{12}\text{C}$ reaction [13] have been found to be in good agreement with the previously measured excitation functions [5]. Typical inclusive energy spectra of α -particles are shown in Fig. 1 at the indicated angles for the $^{28}\text{Si}+^{28}\text{Si}$ reaction at $E_{lab}(^{28}\text{Si}) = 180$ MeV.

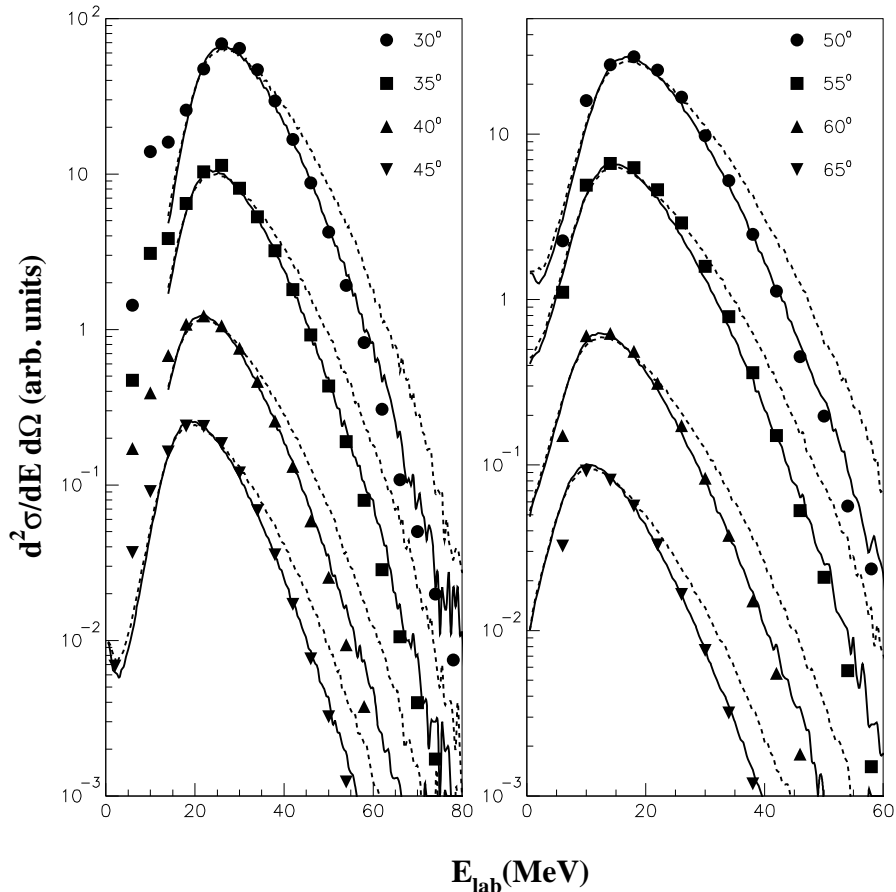


Figure 1: *Energy spectra of α -particles measured in a single mode for the $^{28}\text{Si}(E_{lab} = 180 \text{ MeV}) + ^{28}\text{Si}$ reaction between $\theta_{lab} = 30^\circ$ and 65° . The solid and dashed lines are statistical-model calculations discussed in the text.*

The LCP energy spectra have Maxwellian shapes with an exponential fall-off at high energy (their shape and high-energy slopes are essentially independent of c.m. angle) which reflects a relatively low temperature of the decaying nucleus. This is the signature of a statistical de-excitation process arising from a thermalized source such as the ^{56}Ni CN. Similar LCP spectra have been measured for the lowest bombarding energy. In each case, The sizeable low-energy backgrounds, disappearing in coincidence with ER's (see Fig. 4), arise primarily from binary reaction mechanisms. We have observed the same behavior in the $^{28}\text{Si}+^{12}\text{C}$ reaction for both the α -particles, and the protons at the two incident energies $E_{lab} = 112$ and 180 MeV, in agreement with a previous study at $E_{lab} = 150$ MeV [14], but in strong contrast to previous published data of proton energy spectra that reveal at least a second unexpected component [15].

The velocity contour maps of the invariant cross sections provide an overall picture to characterize the emitting sources with respect to the reaction mechanism. Therefore, to have a better insight into the nature of these emitters, the measured energy spectra of the LCP's have been transformed into invariant cross-section plots in the velocity space. Fig. 2 shows such typical plots of invariant cross-section in the $(V_{\parallel}, V_{\perp})$ plane for α -particles and protons, respectively ; the axes V_{\parallel} and V_{\perp} denote laboratory velocity components parallel and perpendicular to the beam, respectively. The circles are defined to visualize the maxima of intensity production. All spectra can be understood by assuming an evaporative process from a single source, i.e., the thermally equilibrated ^{40}Ca and ^{56}Ni CN's.

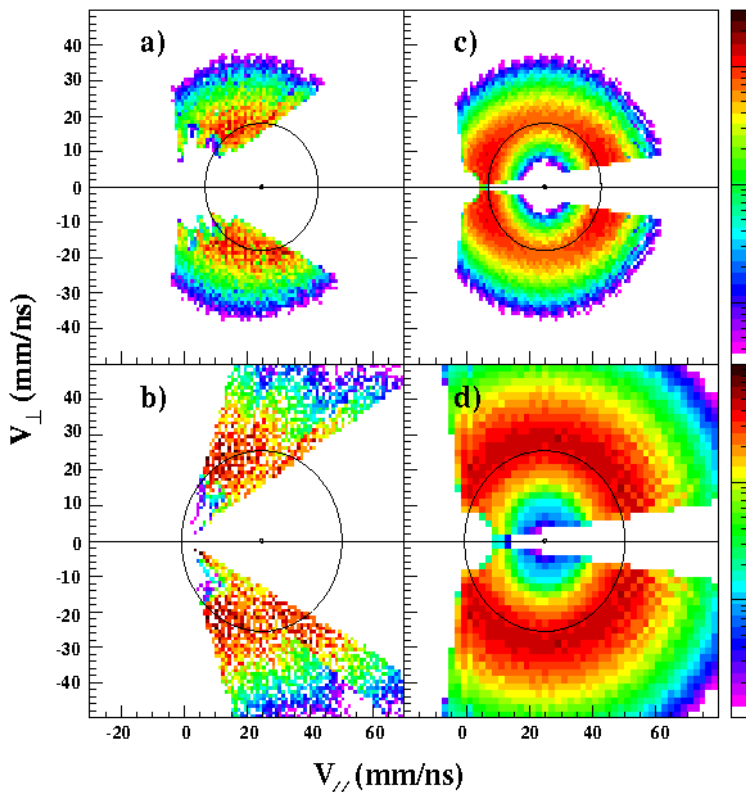


Figure 2: *Inclusive α -particle (a) and proton (b) invariant cross sections measured in the $(V_{\perp}, V_{\parallel})$ plane for the 180 MeV $^{28}\text{Si}+^{12}\text{C}$ reaction. (c) and (d) are statistical-model calculations discussed in the text.*

It is clear from this figure that the invariant cross section contours fall on circles centered at V_{CN} , as expected for a complete fusion-evaporation (CF) mechanism.

The in-plane angular correlation of α -particles in coincidence with all the ER's, produced in the 180 MeV $^{28}\text{Si}+^{12}\text{C}$ reaction, is shown in Fig. 3. The angular correlation is strongly peaked at the opposite side of the ER detector located at $\theta_{lab}^{ER} = -10^\circ$ with respect to the beam. This peaking on the opposite side of the beam is due to the momentum conservation. The solid lines shown in the figure are the results of statistical-model predictions for CF and equilibrium decay using the code CACARIZO, to be discussed in the following

Section. It is seen that the shape of the experimental angular correlations is well reproduced by the theory. However, the excess of yields observed at backward angles ($\theta_{lab} = +50^\circ$ to $+90^\circ$) indicates the occurrence of a non-evaporative process possibly of a binary nature.

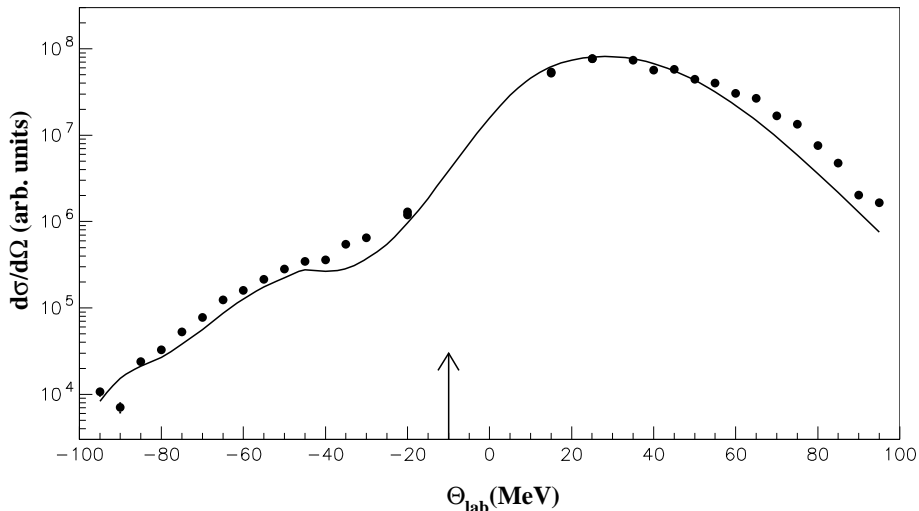


Figure 3: *In-plane 180 MeV $^{28}\text{Si}+^{12}\text{C}$ angular correlations of coincident α -particles. The points correspond to the data, and the solid line to statistical-model calculations discussed in the text. The arrow indicates the position of the IC detector at $\theta_{lab} = -10^\circ$.*

The spectral shapes of the coincident α -particles, displayed in Fig. 5 for the 180 MeV $^{28}\text{Si}+^{12}\text{C}$ reaction are also analysed using the statistical-model code CACARIZO [7,17], as described in the next Section.

III. DISCUSSION

A Hauser-Feshbach [1] analysis of the data has been performed using CACARIZO [7,17], the Monte Carlo version of the statistical-model code CASCADE, in which the experimental geometry of the ICARE detectors is taken into account. The angular momentum distributions needed as the primary input for the calculations were taken from compiled $^{28}\text{Si}+^{12}\text{C}$ [16] and $^{28}\text{Si}+^{28}\text{Si}$ [18] CF data, respectively. The other standard ingredients for statistical-model calculations, namely the nuclear level densities and the barrier transmission probabilities, are obtained from studies of the evaporated LCP spectra. In recent years, it has been observed that the standard statistical model cannot predict satisfactorily the shape of the evaporated α -particle energy spectra [7-11], and the calculated average energies of the α -particles are found to be much higher than the corresponding experimental results. Several attempts have been made to explain this anomaly either by changing the emission barrier or by using spin-dependent level densities. Adjusting the emission barriers and corresponding transmission probabilities affect the lower energy part of the calculated evaporation spectra. On the other hand the high-energy part of the spectra depends crucially on the available phase space obtained from the level densities at high spin. In hot rotating nuclei formed in heavy-ion reactions, the energy level density at higher angular momentum is spin dependent.

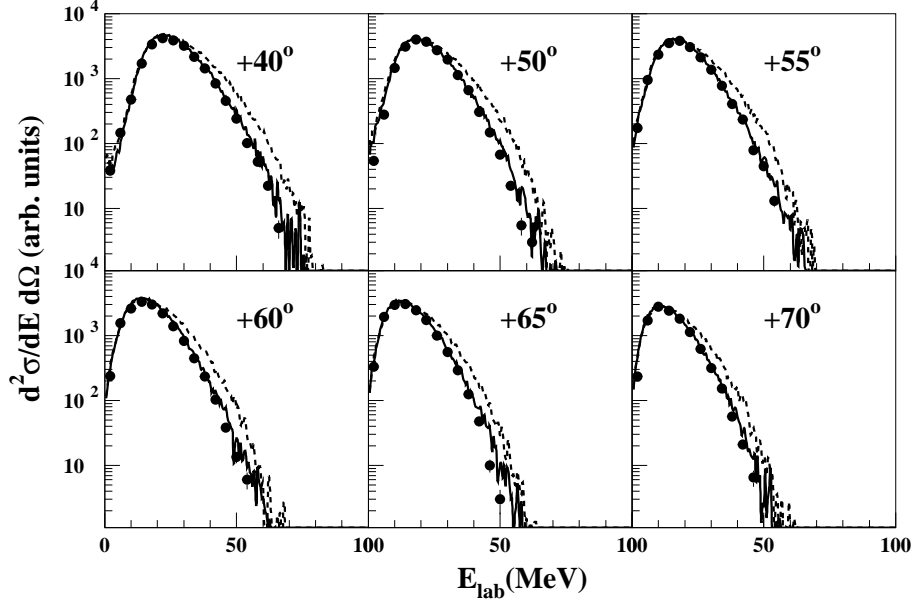


Figure 4: *Exclusive energy spectra of α -particles emitted in coincidence with all ER's detected at -10° , at the indicated laboratory angles, in the 180 MeV $^{28}\text{Si}+^{28}\text{Si}$ reaction. The solid and dashed lines are statistical-model calculations discussed in the text.*

The level density, $\rho(E, J)$, for a given angular momentum J and energy E is given by the well known Fermi gas expression :

$$\rho(E, J) = \frac{(2J+1)}{12} a^{1/2} \left(\frac{\hbar^2}{2\mathcal{J}_{eff}} \right)^{3/2} \frac{1}{(E - \Delta - t - E_J)^2} \exp(2[a(E - \Delta - t - E_J)]^{1/2}) \quad (1)$$

where a is the level density parameter, t is the “nuclear” temperature and Δ is the pairing correction, $E_J = \frac{\hbar^2}{2\mathcal{J}_{eff}} J(J+1)$ is the rotational energy, $\mathcal{J}_{eff} = \mathcal{J}_0 \times (1 + \delta_1 J^2 + \delta_2 J^4)$ is the effective moment of inertia, \mathcal{J}_0 is the rigid body moment of inertia and δ_1 and δ_2 are deformability parameters [7,8,10,11]. By changing the deformability parameters δ_1 and δ_2 one can simulate the spin-dependent level density [7,8]. The CACARIZO calculations have been performed using two sets of input parameters : the first one with standard rotating liquid drop model (RLDM) [1] parameters, and the second one with non-zero values for the deformability parameters [13,19,20,21] which are listed in Table I.

For the 180 MeV $^{28}\text{Si} + ^{28}\text{Si}$ reaction, the shape of the inclusive (see Fig. 1) and exclusive (see Fig. 4) α energy spectra are well reproduced by using deformation effects [13,19,20,21]. The dashed lines in Figs. 1 and 4 show the predictions of CACARIZO using the standard RLDM deformation parameter set with no extra deformation ($\delta_1 = \delta_2 = 0$). It is clear that the average energies of the measured α energy spectra are lower than those predicted by the standard statistical-model calculations. The solid lines show the predictions

Reaction	C.N.	Energy [MeV]	l_{cr} [\hbar]	δ_1	δ_2	b/a	β_2	Reference
$^{28}\text{Si}+^{28}\text{Si}$	^{56}Ni	111.6 and 180	34 and 37	$1.2\cdot 10^{-4}$	$1.1\cdot 10^{-7}$	1.6 and 1.7	.49 and .50	This work
$^{28}\text{Si}+^{12}\text{C}$	^{40}Ca	111.6 and 180	21 and 27	$2.5\cdot 10^{-4}$	$5.0\cdot 10^{-7}$	1.7 and 1.8	.47 and .51	This work
$^{28}\text{Si}+^{12}\text{C}$	^{40}Ca	150	26	$6.5\cdot 10^{-4}$	$3.3\cdot 10^{-7}$	1.7	.51	[5]
$^{35}\text{Cl}+^{24}\text{Mg}$	^{59}Cu	260	37	$1.1\cdot 10^{-4}$	$1.3\cdot 10^{-7}$	1.4 to 2.0	.46 to .53	[22]
$^{32}\text{S}+^{27}\text{Al}$	^{59}Cu	100 to 150	27 to 39	$2.3\cdot 10^{-4}$	$1.6\cdot 10^{-7}$	2.0	.53	[7]
$^{32}\text{S}+^{27}\text{Al}$	^{59}Cu	100 to 150	27 to 42	$1.3\cdot 10^{-4}$	$1.2\cdot 10^{-7}$	1.5 to 2.2	.48 to .54	[10]
$^{28}\text{Si}+^{27}\text{Al}$	^{55}Co	150	42	$1.8\cdot 10^{-4}$	$1.8\cdot 10^{-7}$	1.3	.46	[11]

Table 1: *Input parameters of the CACARIZO calculations.*

of CACARIZO using the parameter set with $\delta_1 = 1.2 \times 10^{-4}$ and $\delta_2 = 1.1 \times 10^{-7}$ chosen to reproduce the data consistently at the two bombarding energies. The shapes of the inclusive as well as the exclusive α energy spectra are well described after including these significant deformation effects. CACARIZO calculations of the invariant cross sections, plotted in Fig. 2, reproduce well the data obtained in the 180 MeV $^{28}\text{Si}+^{12}\text{C}$ reaction for both α -particles and protons, respectively. In this case the CACARIZO parameters are similar to those employed in a previous study of the 130 MeV $^{16}\text{O}+^{24}\text{Mg}$ reaction [17], with the use of the angular momentum dependent level densities. The exclusive energy spectra of α -particle measured in coincidence with individual S and P ER's, which are shown in Fig. 5 for $E_{lab} = 180$ MeV, are quite interesting. The energy spectra associated with S are completely different from those associated with P [13]. The latter are reasonably well reproduced by the CACARIZO curves whereas the model could not predict the shape of the spectra obtained in coincidence with S at backward angle ($\theta_\alpha \geq 70^\circ$). Additional non-statistical components appear to be significant in this case. This is consistent with the discrepancies also observed at backward angles in the in-plane angular correlations of Fig. 3. The same observations can be made at the lower bombarding energy $E_{lab} = 112$ MeV [19-21]. We will show that the hypothesis of a contributions arising from the decay of unbound ^8Be clusters produced in a binary reaction $^{40}\text{Ca} \rightarrow ^{32}\text{S}+^8\text{Be}$ is consistent with the experimental results.

In Fig. 6 the energies of the α -particles (detected in coincidence with the S residues at the indicated angles) are plotted against the energies of the S residues detected at $\theta_S = -10^\circ$. At $\theta_\alpha = +40^\circ, +45^\circ$ and $+50^\circ$ the main bulk of events are from a statistical origin, and consistent with CACARIZO calculations (see Fig. 7). For larger angles, the two branches, labelled 1 and 2, are outside the "statistical evaporation region", but still correspond to a evaporation process as shown by the CACARIZO calculations displayed in Fig. 7. This two branches 1 and 2 corresponds to a 2- α channel with both α -particles emitted respectively at backward and forward angles in the center of mass.

However, at more backward angles other contributions, labelled 3 and 4, appear more and more significantly. The observed "folding angles" are compatible with the two-body kinematics required for the $^{32}\text{S}+^8\text{Be}$ binary exit-channel. On the other hand, the energy correlations for the α -particles in coincidence with the P residues (not shown) do not exhibit any of the two-body branches and, thus, the "statistical evaporation region" alone, which is consistent with the CACARIZO predictions at all the measured angles, appears significantly.

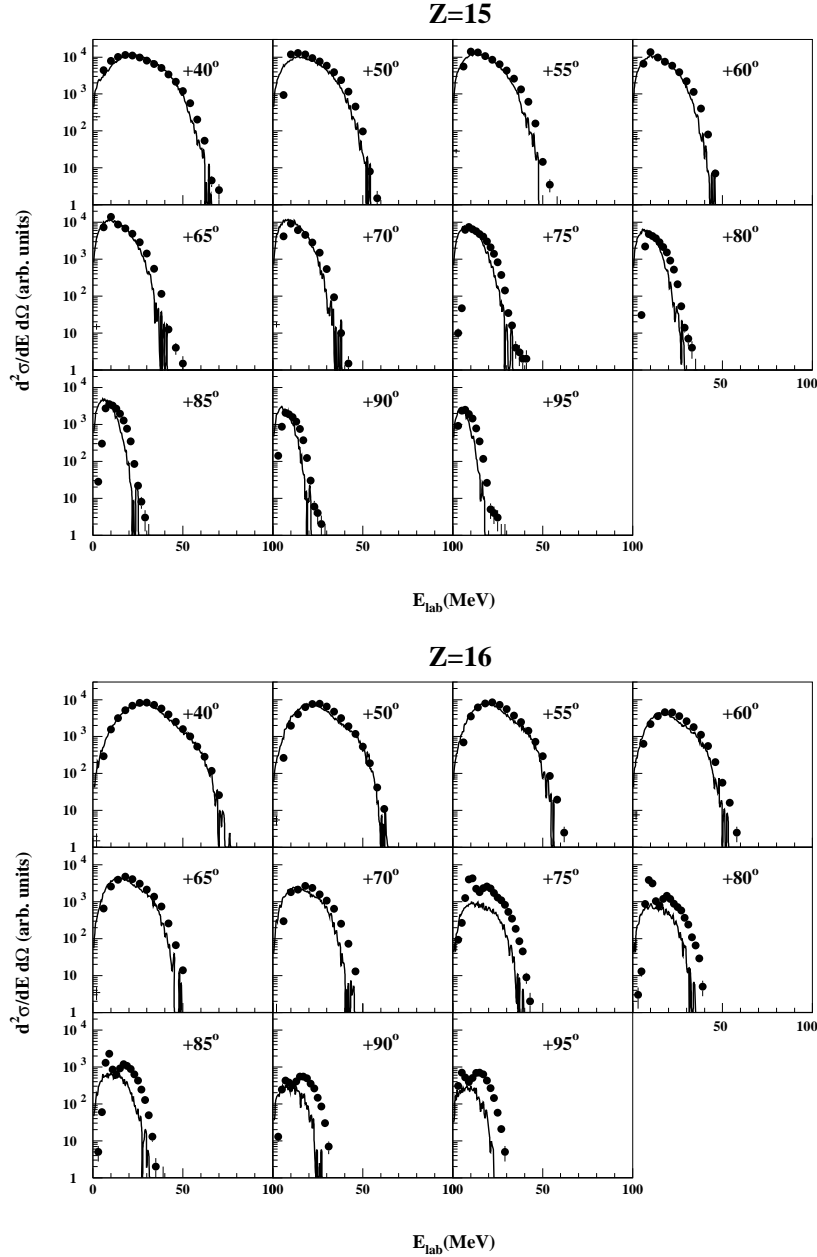


Figure 5: *Exclusive energy spectra of α -particles emitted in coincidence with individual P and S ER's detected at -10° , at the indicated laboratory angles, in the 180 MeV $^{28}\text{Si}+^{12}\text{C}$ reaction. The solid lines are statistical-model calculations discussed in the text.*

In the left side of Fig. 8 the excitation energy of ^8Be , calculated by assuming a two-body process, is presented for the contributions labelled 2, 3, and 4 (Fig. 6) at different indicated angles. From 55° to 95° the main bulk of the yields is centered at around 3.06 ± 1.50 MeV, the energy of the first 2^+ excited level of ^8Be ; whereas, from 70° to 90° a second component is centered at the energy of the ground state of ^8Be (squared part). This last

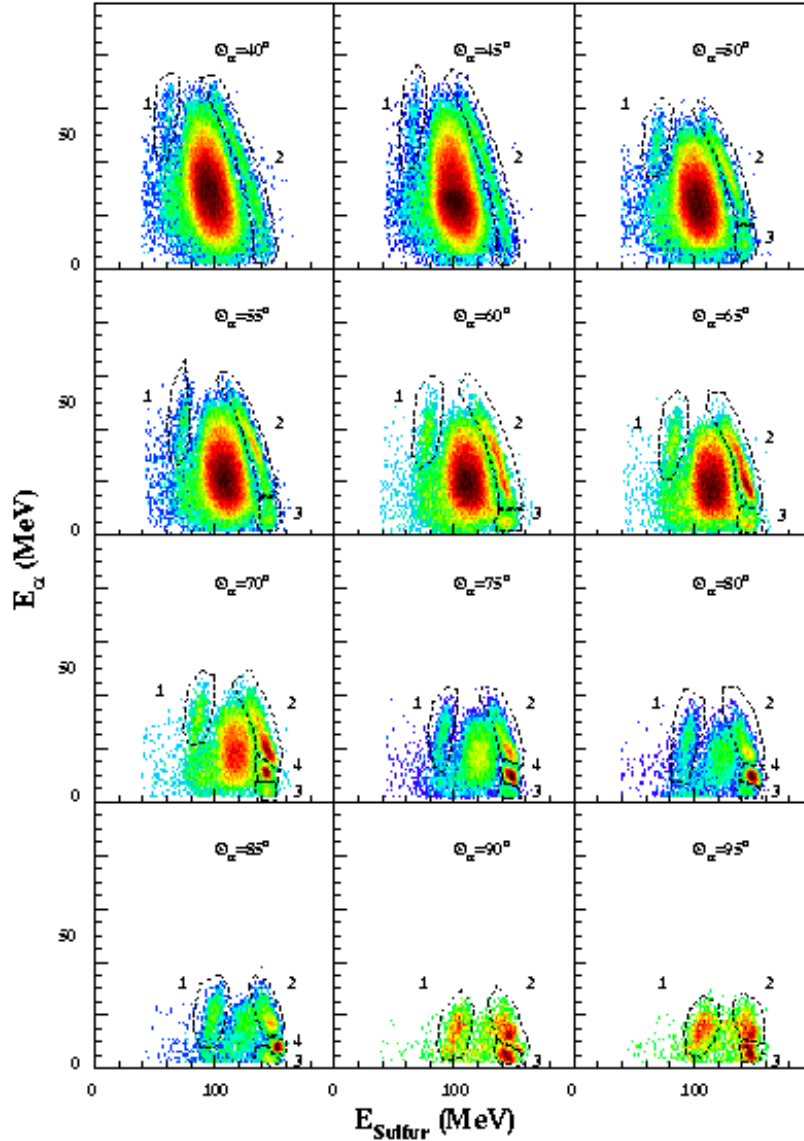


Figure 6: Energy-correlation plots between coincident α -particles and S ER's produced in the 180 MeV $^{28}\text{Si}+^{12}\text{C}$ reaction. The heavy fragments is detected at $\theta_S = -10^\circ$ and α 's angles are given in the figure. The dashed lines correspond to different contours and their associated labelling are discussed in the text.

component corresponds to the contribution 4 (Fig. 6). Fusion-fission calculations using the Extended Hauser-Feshbach Method [3] fail to reproduce both the excitation energies of the S residue, and the yields from the 3 and 4 contributions [12]. However, these contributions can be interpreted as due to an incomplete fusion (ICF) process governed by a α -transfer reaction mechanism $^{28}\text{Si}+^{12}\text{C} \rightarrow ^{32}\text{S}^*+^8\text{Be}$ as proposed by Morgenstern *et al.* [23]. This conclusion is in agreement with previous inclusive results published in Ref. [24]. In the cluster-transfer picture the reaction is characterized by a "Q-value" window" centered at the so-called "Q-optimum", which value can be estimated semi-classically by $Q_{opt} = (Z_3Z_4/Z_1Z_2-$

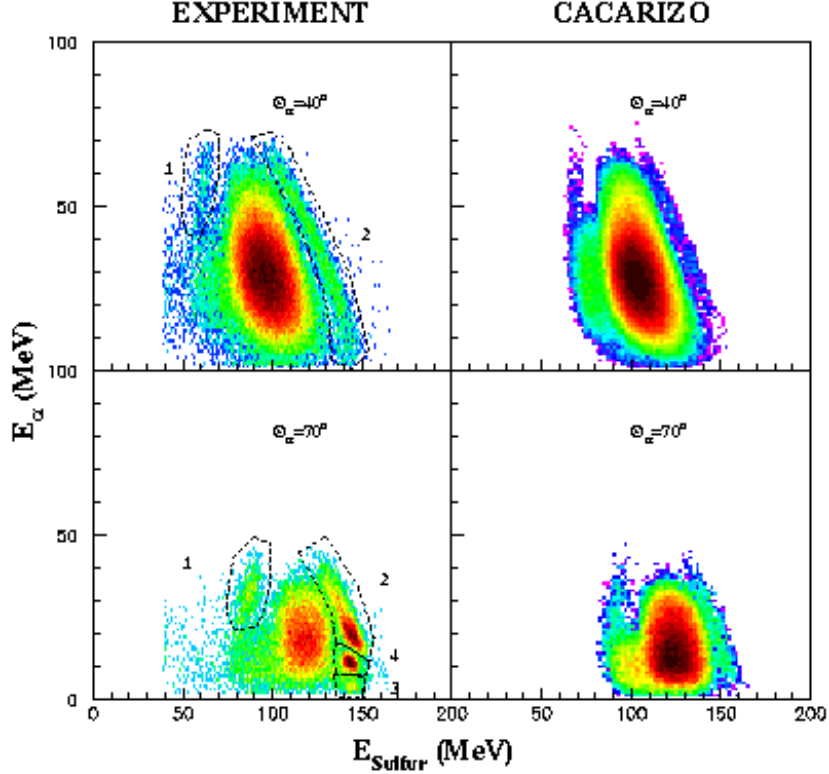


Figure 7: *Experimental and calculated energy-correlation plots between coincident α -particles and S ER's produced in the 180 MeV $^{28}\text{Si}+^{12}\text{C}$ reaction. The S is detected at $\theta_S = -10^\circ$ and α 's at $\theta_\alpha = +40^\circ$, and $+70^\circ$, respectively. CACARIZO calculations are discussed in the text.*

1) $E_i^{c.m.}$, where the indices 1,2 and 3,4 indicate the entrance (i) and exit channel, respectively. The corresponding excitation energy $E^* = Q_{gg} - Q_{opt}$, with Q_{gg} is the ground-state Q-value of the reaction. In this case the expected excitation energy in the ^{32}S nuclei is equal to 12.9 MeV. The right hand side of Fig. 8 represents the calculated excitation energy of ^{32}S in coincidence with the ground state (g.s), and with the first excited state of ^8Be , respectively. The dashed lines correspond to $E^{**} = 12.9$ MeV, the energy expected for a α -transfer reaction mechanism. In both cases the excitation energies of ^{32}S are consistent with these values.

To summarize, the properties of the emitted LCP's in the $^{28}\text{Si} + ^{12}\text{C}, ^{28}\text{Si}$ reactions, which are reasonably well described by statistical-model calculations using spin-dependent level densities, suggest significant deformation effects at high spin for the ^{40}Ca and ^{56}Ni dinuclear systems. In the case of $^{28}\text{Si} + ^{12}\text{C}$ the α -particle energy spectra measured in coincidence with a S residue exhibits an additional component arising from the cluster decay of the unbound ^8Be nucleus, produced through the α -cluster-transfer of $^{40}\text{Ca} \rightarrow ^{32}\text{S} + ^8\text{Be}$. This type of reaction allows to populate some N=Z nuclei with a well defined excitation energy. Thus, sophisticated particle- γ experiments (see Refs. [25-28] for instance) using EUROBALL IV and/or GAMMASPHERE should be performed in the very near future in

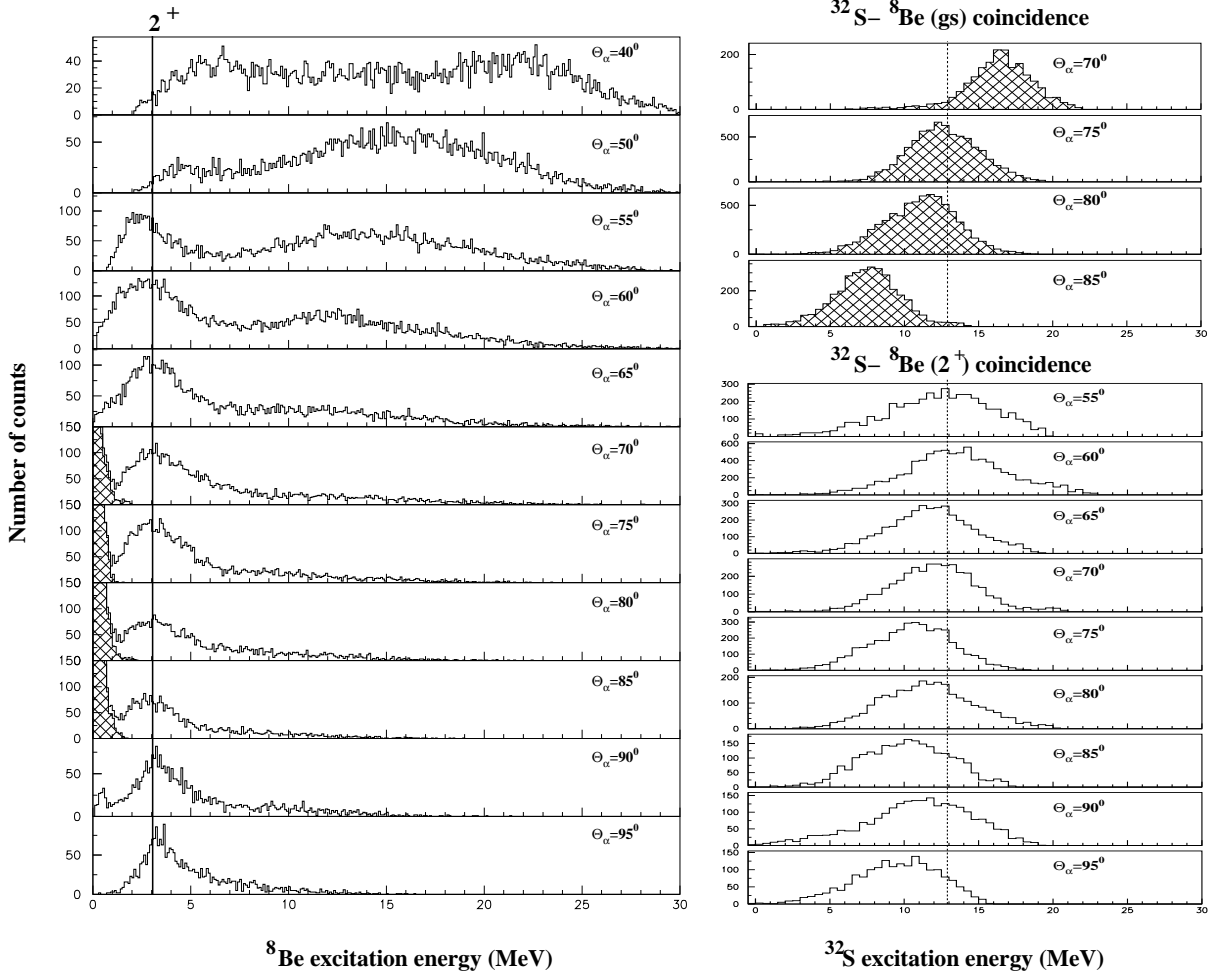


Figure 8: *Calculated excitation energy spectra for ${}^8\text{Be}$ (left) and ${}^{32}\text{S}$ (right) in coincidence with the g.s. (up) and first excited level (down) of ${}^8\text{Be}$. The solid line corresponds to the energy of the first excited state of ${}^8\text{Be}$ (3.06 MeV). the dashed lines correspond to ${}^{32}\text{S}$ excitation energy expected for an α -transfer process.*

order to well define and understand what are the best types of reaction which are capable to populate significantly the superdeformed bands discovered and/or predicted in this mass region.

Acknowledgements : This paper is based upon the Ph.D. Thesis of Marc Rousseau, Université Louis Pasteur, Strasbourg, 2000. We would like to thank the staff of the VIVITRON for the excellence support in carrying out these experiments. M.R. would like to acknowledge the Conseil Régional d’Alsace for the financial support of his Ph.D. Thesis work. Parts of this work has also been done in collaboration with C.E. during his summer stay at IReS with a JANUS Grant of IN2P3.

References :

- [1] S.J. Sanders, A. Szanto de Toledo, and C. Beck, Phys. Rep. **311**, 487 (1999).
- [2] S.J. Sanders, Phys. Rev. C **44**, 2676 (1991).
- [3] T. Matsuse *et al.*, Phys. Rev. C **55**, 1380 (1997).
- [4] B. Shivakumar *et al.*, Phys. Rev. C **35**, 1730 (1987).
- [5] D. Shapira *et al.*, Phys. Lett. **114B**, 111(1982); *ibidem*, Phys. Rev. Lett. **53**, 1634 (1984)
- [6] C.E. Svensson *et al.*, Phys. Rev. Lett. **85**, 2693 (2000); R.V.F. Janssens, private communication
- [7] G. Viesti *et al.*, Phys. Rev. C **38**, 2640 (1988) and references therein.
- [8] I.M. Govil *et al.*, Phys. Lett. B **197**, 515 (1987).
- [9] G. La Rana *et al.* Phys. Rev. C **37**, 1920 (1988); *ibidem* C **40**, 2425 (1989).
- [10] J. R. Huizenga *et al.*, Phys. Rev. C **40**, 668 (1989).
- [11] I.M. Govil *et al.*, Nucl. Phys. **A674**, 377 (2000); *ibidem*, Phys. Rev. C **57**, 1269 (1998); *ibidem*, Phys. Lett. **B307**, 283 (1993).
- [12] M. Rousseau, Ph.D. Thesis, Université Louis Pasteur, Strasbourg (2000); IReS Report **01-02**.
- [13] C. Beck *et al.*, Ricerca Scientifica ed Educazione Permanente (Supp.) **115**, 407 (2000).
- [14] M. Kildir *et al.*, Phys. Rev. C **51**, 1873 (1995).
- [15] S.K. Hui *et al.*, Nucl. Phys. **A641**, 21 (1998); Erratum **A645**, 605 (1999).
- [16] M.F. Vineyard *et al.*, Phys. Rev. C **47**, 2374 (1993).
- [17] B. Fornal *et al.*, Phys. Rev. C **44**, 2588 (1991).
- [18] M.F. Vineyard *et al.*, Phys. Rev. C **41**, 1005 (1990).
- [19] C. Bhattacharya *et al.*, Nucl. Phys. **A654**, 841c (1999); *ibidem*, Phys. Rev. C (in preparation).
- [20] M. Rousseau *et al.*, Clustering Aspects of Nuclear Structure and Dynamics, eds. M. Korolija, Z. Basrak and R. Caplar (World Scientific Publishing Co., Singapore, 2000), p.189.
- [21] C. Bhattacharya *et al.*, Pramana (Indian Journal of Physics), to be published (2001); IReS Report **00-19**.
- [22] D. Mahboub, Ph.D. Thesis, Université Louis Pasteur, Strasbourg (1996); CRN Report **96-36**.
- [23] H. Morgenstern *et al.*, Z. Phys. A **324**, 443 (1986).
- [24] N. Arena *et al.*, Phys. Rev. C **50**, 880 (1994).
- [25] R. Nouicer *et al.*, Phys. Rev. C **60**, 41303 (1999).
- [26] C. Beck *et al.*, Phys. Rev. C **63**, 014607 (2001).
- [27] S. Thummerer *et al.*, Phys. Scr. **T88**, (2000).
- [28] S. Thummerer *et al.*, Jour. of Phys. (London) **G**(2001), to be published.